iScience

CellPress
OPEN ACCESS

Article

N6-methyladenosine-associated genetic variants in NECTIN2 and HPCAL1 are risk factors for abdominal aortic aneurysm

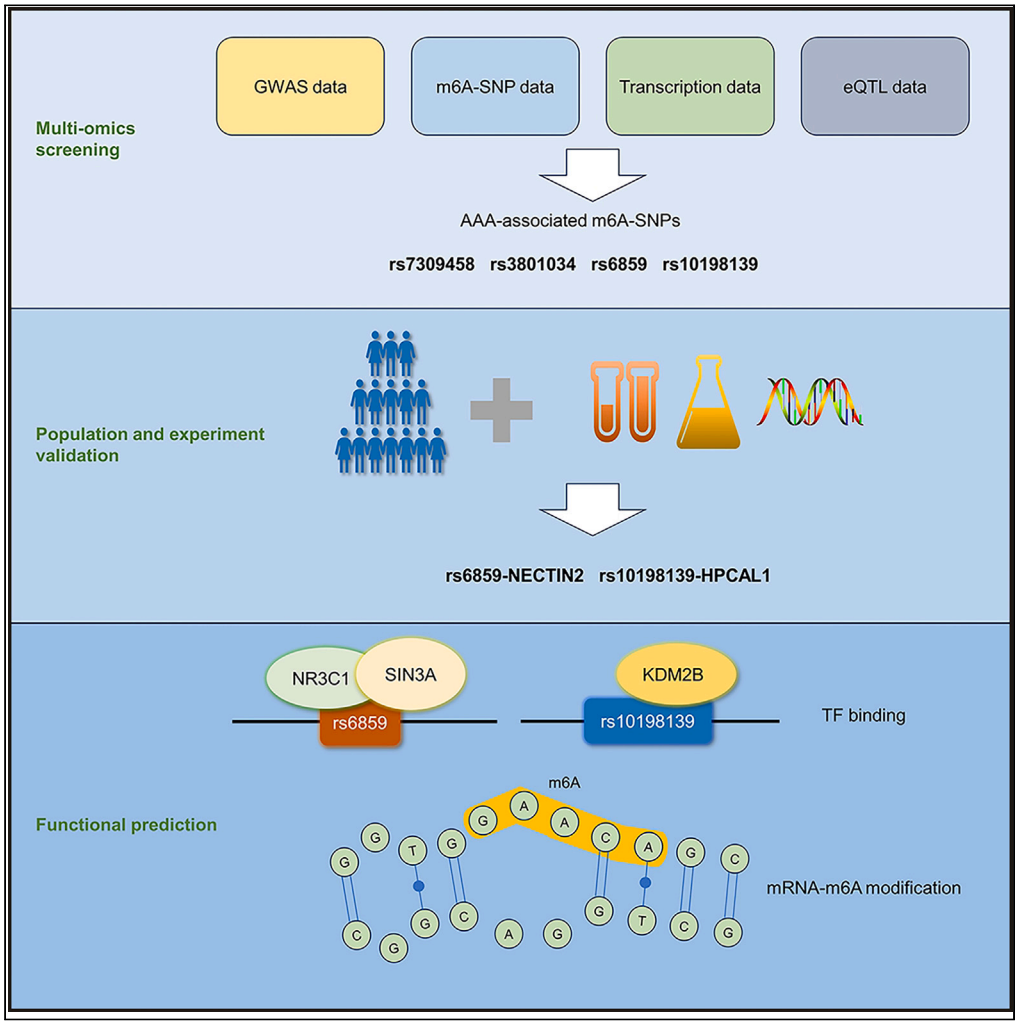

Tan Li, Yijun Wu, Jun Yang, Jingjing Jing, Chunyan Ma, Liping Sun

macy@cmu1h.com (C.M.)
lpsun@cmu.edu.cn (L.S.)

Highlights

Two m6A-SNPs, NECTIN2 rs6859, and HPCAL1 rs10198139, are associated with AAA risk

Inclusion of rs6859 and rs10198139 enhances the predictive efficiency of AAA risk

The identified SNPs may regulate local gene expression via an m6A-mediated manner

Li et al., iScience 27, 109419
April 19, 2024
https://doi.org/10.1016/j.isci.2024.109419

iScience

CellPress
OPEN ACCESS

Article

N6-methyladenosine-associated genetic variants in NECTIN2 and HPCAL1 are risk factors for abdominal aortic aneurysm

Tan Li,[1,2,5] Yijun Wu,[3,4,5] Jun Yang,[1,2] Jingjing Jing,[3,4] Chunyan Ma,[1,2,*] and Liping Sun[3,4,6,*]

SUMMARY

Although N6-methyladenosine (m6A) modification has been implicated in the pathogenesis of abdominal aortic aneurysm (AAA), the relationship between m6A-associated single nucleotide polymorphisms (m6A-SNPs) and AAA remains unknown. This study used integrative multi-omics analysis and clinical validation approaches to systematically identify potential m6A-SNPs connected with AAA risk. We found that rs6859 and rs10198139 could modulate the expression of local genes, NECTIN2 and HPCAL1, respectively, which exhibited upregulation in AAA tissues, and their risk variants were significantly correlated with an increased susceptibility to AAA. Incorporating rs6859 and rs10198139 improved the efficiency of AAA risk prediction compared to the model considering only conventional risk factors. Additionally, these two SNPs were predicted to be located within the regulatory sequences, and rs6859 showed a substantial impact on m6A modification levels. Our findings suggest that m6A-SNPs rs6859 and rs10198139 confer an elevated risk of AAA, possibly by promoting local gene expression through an m6A-mediated manner.

INTRODUCTION

Abdominal aortic aneurysm (AAA) is a multifactorial vascular disorder featured by the localized and irreversible weakening and dilation of the abdominal aorta. Several well-established risk factors for AAA have been identified, including advanced age, male sex, smoking status, hypertension, and dyslipidemia.[1,2] Furthermore, extensive research has highlighted the significant role of genetic factors in the onset and progression of AAA.[3,4] Despite numerous candidate gene association studies conducted, most of them have not been replicated in independent cohorts, indicating the need for further investigation and validation.[5]

Recently, genome-wide association study (GWAS) has emerged as a powerful tool for uncovering genetic risk variants relevant to complex trait diseases in a hypothesis-free approach, which reveals a multitude of chromosomal regions.[4,6] In the context of AAA, GWAS has identified a large number of single nucleotide polymorphisms (SNPs) specific to AAA in both protein-coding and non-protein-coding regions.[7,8] These AAA-specific SNPs and their associated genes have been found to modulate extracellular matrix organization, inflammation, lipid metabolism, oxidative stress, and smooth muscle cell function, suggesting that part of these AAA pathological traits could stem from genetic abnormalities.[9] Genetic regulation of gene expression has been fully described in many human tissue types, and expression quantitative trait loci (eQTLs) seem to underlie a considerable fraction of variant-trait associations.[10] Mapping of eQTLs has been conducted to associate SNPs with risk genes in vascular cells and tissues.[11–13] However, the impact of genetic variants on epigenetic alterations in human complex diseases, including AAA, remains largely uncharacterized.

Over the past decade, substantial work has been performed on the mechanisms of epigenetic regulation in cardiovascular field. N6-methyladenosine (m6A) becomes the most prevalent post-transcriptional modification in eukaryotic messenger RNA (mRNA) and may participate in a plenty of human diseases.[14] The m6A modification site can recruit specific protein complexes, thereby regulating the structure, function and stability of mRNA, and modulating the gene expression or splicing.[15,16] It has been confirmed that certain SNPs within or near m6A motifs may influence the methylation levels of m6A and fundamental biological activities by altering the RNA sequences of target sites or key flanking nucleotides, and these SNPs are referred to as m6A-associated SNPs (m6A-SNPs).[17–19] To date, m6A-SNPs have been found to be implicated in a variety of disorders such as coronary artery disease, ischemic stroke, and breast cancer.[16,20–22]

[1]Department of Cardiovascular Ultrasound, the First Hospital of China Medical University, Shenyang 110001, China
[2]Clinical Medical Research Center of Imaging in Liaoning Province, the First Hospital of China Medical University, Shenyang 110001, China
[3]Tumor Etiology and Screening Department of Cancer Institute and General Surgery, the First Hospital of China Medical University, Shenyang 110001, China
[4]Key Laboratory of Cancer Etiology and Prevention in Liaoning Education Department, the First Hospital of China Medical University, Shenyang 110001, China
[5]These authors contributed equally
[6]Lead contact
*Correspondence: macy@cmu1h.com (C.M.), lpsun@cmu.edu.cn (L.S.)
https://doi.org/10.1016/j.isci.2024.109419

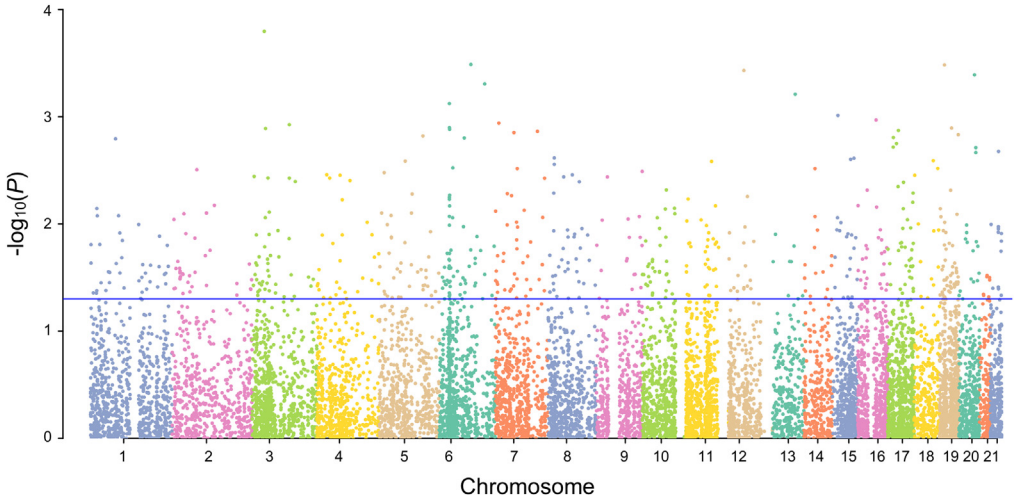

Figure 1. The Manhattan plot of 11,601 m6A-SNPs in the context of aortic aneurysm

The horizontal axis represents the chromosome position, and the vertical axis indicates the -$\log_{10}(P)$ value. The blue line indicates the p value of 0.05, and m6A-SNPs above the line are considered to be associated with aortic aneurysm. Each point on the plot represents a single m6A-SNP.

The significance of m6A methylation in AAA has been reported, with abnormal m6A modification levels contributing to disturbed RNA metabolism and aberrant gene expression closely linked to AAA incidence and progression.[23–25] However, the correlation between m6A-SNPs and AAA risk in the human population remains unclear. Identifying AAA-associated m6A-SNPs through large-scale GWAS is crucial for understanding the genetic mechanisms underlying m6A modification in AAA pathogenesis and improving the fine mapping of causal variants.

Here, we employed an integrative analysis method to screen potential m6A-SNPs associated with AAA by mining publically available SNP association data from GWAS, differential expression data from the Gene Expression Omnibus (GEO) and our sequencing results, along with a list of m6A-SNPs with eQTLs. Then, we validated the expression of selected genes and effects of candidate m6A-SNPs on AAA risk through case-control studies. Additionally, efforts were made to perform functional predictions on the identified SNPs. This investigation aims to provide insights into the connection between m6A-SNPs and AAA and facilitate the translation of gene research findings into new therapeutic targets.

RESULTS

Identification of m6A-SNPs in aortic aneurysm

We analyzed a total of 13,435,467 SNPs from the GWAS summary data of aortic aneurysm (PheWeb: aortic aneurysm), as well as 1,401,814 human m6A-SNPs from the RMVar: RMVar_Human_basic_info_m6A. After taking the intersection and removing the X chromosomes loci, we identified a total of 11,601 m6A-SNPs in 6720 genes, and among them, 622 m6A-SNPs were found to be associated with aortic aneurysm ($p < 0.05$) (Figure 1). The number of m6A-SNPs with high confidence levels from miCLIP/m6A-REF-seq/m6ACE-seq/DART-seq/PA-m6A-seq was 3,832, while the medium-level SNPs from MeRIP-seq and m6A-Seal-seq experiments were 2,520, and low-level SNPs based on a deep convolutional neural network were 5,249.

Identification of DEGs containing m6A-SNPs associated with AAA

We focused on m6A-SNPs situated in the gene body region to analyze differential gene expression, and 2,237 m6A-SNPs from non-intergenic regions in 1,622 genes were obtained according to location annotation. In order to determine the resulting list of AAA-related m6A-SNPs, we utilized transcriptomic expression profile data specific to AAA disease. A comparison between human AAA and control aortic tissues revealed 404 differentially expressed genes (DEGs) from the GEO: GSE7084 and 928 DEGs from our RNA-seq data. Volcano plots were generated using SangerBox, as shown in Figures 2A and 2B. After taking the intersection, a total of 170 DEGs containing 228 m6A-SNPs were detected (Figure 2C) (Table S2). The results of gene ontology (GO) and Kyoto encyclopedia of genes and genomes (KEGG) analysis of 170 m6A-SNP containing genes are shown in Figures 2D and 2E, displaying the top 5 biological processes and signaling pathways relevant to AAA.

Analysis of eQTL in m6A-SNPs and gene expression validation

Out of the 228 m6A-SNPs within above DEGs, 12 were found to be significantly associated with AAA risk ($p < 0.05$). We performed eQTL analysis using VannoPortal to explore whether these 12 m6A-SNPs were linked to local gene expression. As a result, we identified four m6A-SNPs, namely rs7309458, rs3801034, rs6859, and rs10198139, which exhibited *cis*-eQTL signals and had a significant correlation with

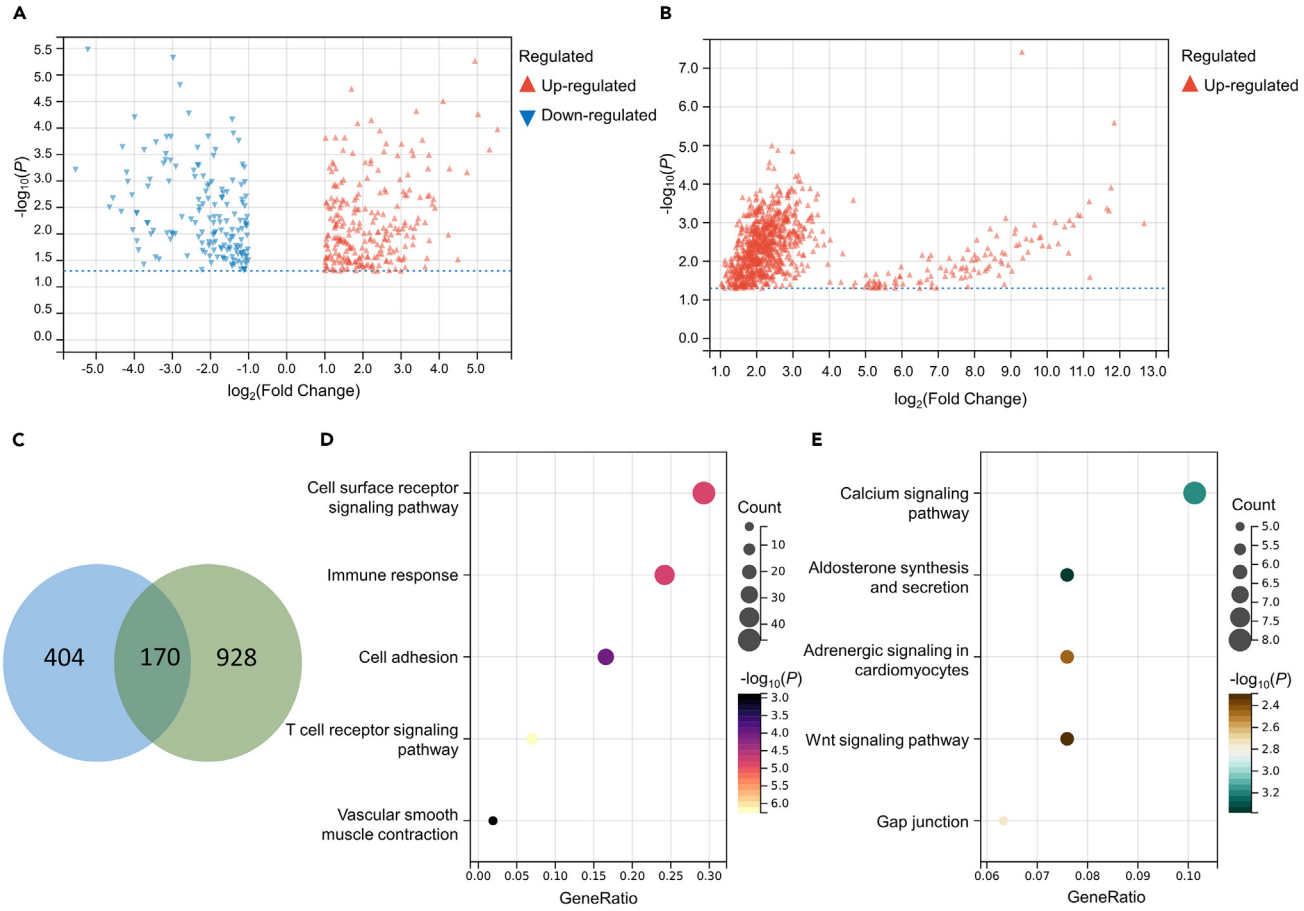

Figure 2. Identification and enrichment analysis of DEGs containing m6A-SNPs between AAA and control tissues based on the shared DEG list

The volcano plot of DEGs containing m6A-SNP from the GEO: GSE7084 (A) and our RNA-seq data (B). The horizontal axis represents the $\log_2$(Fold Change) value, and the vertical axis represents the $-\log_{10}(P)$ value. Red color indicates up-regulated genes, and Blue color indicates down-regulated genes in human AAA tissues. (C) The venn diagram of DEGs obtained from the intersection of GEO: GSE7084 and sequencing data. See also Table S2. GO (D) and KEGG (E) analysis reveals 5 biological processes and signaling pathways relevant to AAA, respectively. The size of each point represents the number of genes associated with the corresponding biological process or pathway, and the color intensity reflects the $-\log_{10}(P)$ value.

the expression of local genes-OSBPL8, ZNF12, NECTIN2, and HPCAL1, respectively. Additionally, two m6A-SNPs (rs7309458 and rs3801034) showed *trans*-eQTL signals and were associated with the expression of other genes. Ultimately, the four SNPs with *cis*-eQTL signals were chosen due to the regulatory impact of m6A modification on nearby gene expression. Detailed functional information for these SNPs has been provided in Table 1.

The mRNA levels of previous four DEGs based on the GSE7084 dataset and RNA-seq data are presented in Figures 3A and 3B. To further validate the expression of these four genes in AAA and control tissues, we performed mRNA-level validation using our clinical samples. The qRT-PCR results demonstrated a significant upregulation of OSBPL8, NECTIN2, and HPCAL1 expression in AAA tissues compared to control aortas (all $p < 0.05$) (Figure 3C). Thus, three m6A-SNPs formed an SNP-gene expression-AAA triplet. Considering the racial disparities of SNPs, we further screened for SNPs with a minor allele frequency (MAF) > 0.1 in the Asian population, and rs7309458 was excluded. Therefore,

Table 1. The information of four AAA-associated m6A-SNPs with *cis*-eQTL signals

Variant	CHR	Position	Mutation type	p value	Gene	TF bound	Motifs changed	m6A ID	m6A function
rs7309458	12	76760920	intron	0.015	OSBPL8	Yes	Yes	RMVar_ID_187184	Loss
rs3801034	7	6734141	intron	0.036	ZNF12	Yes	Yes	RMVar_ID_700874	Loss
rs6859	19	45382034	3′-UTR	0.039	NECTIN2	Yes	Yes	RMVar_ID_455409	Loss
rs10198139	2	10515770	intron	0.040	HPCAL1	Yes	Yes	RMVar_ID_389223	Loss

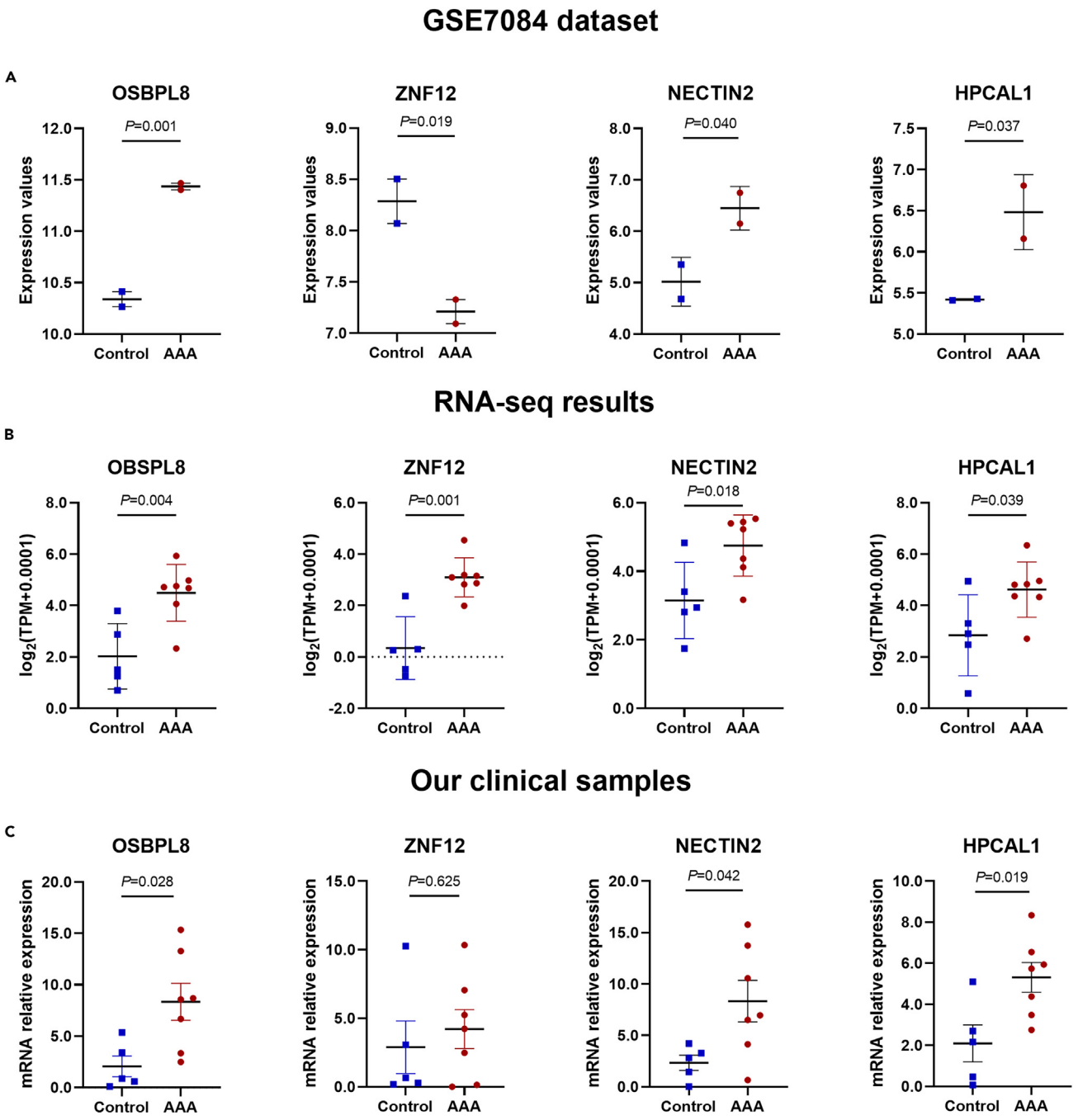

Figure 3. The regional association maps of rs6859 and rs10198139

The scatterplot graphs of four DEGs based on the GEO: GSE7084 (A), RNA-seq results (B) and our clinical samples (C). The mRNA expression levels of OSBPL8, NECTIN2, and HPCAL1 exhibit significant upregulation in AAA tissues as compared with control aortas (all $p < 0.05$). See also Table S1.

rs6859 and rs10198139 have the potential to be implicated in the occurrence of AAA by influencing local gene expression through m6A modification.

The entire screening process and results of candidate m6A-SNPs associated with AAA risk are presented in Figure 4.

Association between candidate m6A-SNPs and AAA risk in our study population

Baseline characteristics of our study population are shown in Table 2. There were no significant differences in the distribution of age, sex, smoking status, and diabetes. AAA patients had a significantly higher proportion of hypertension and dyslipidemia compared to controls

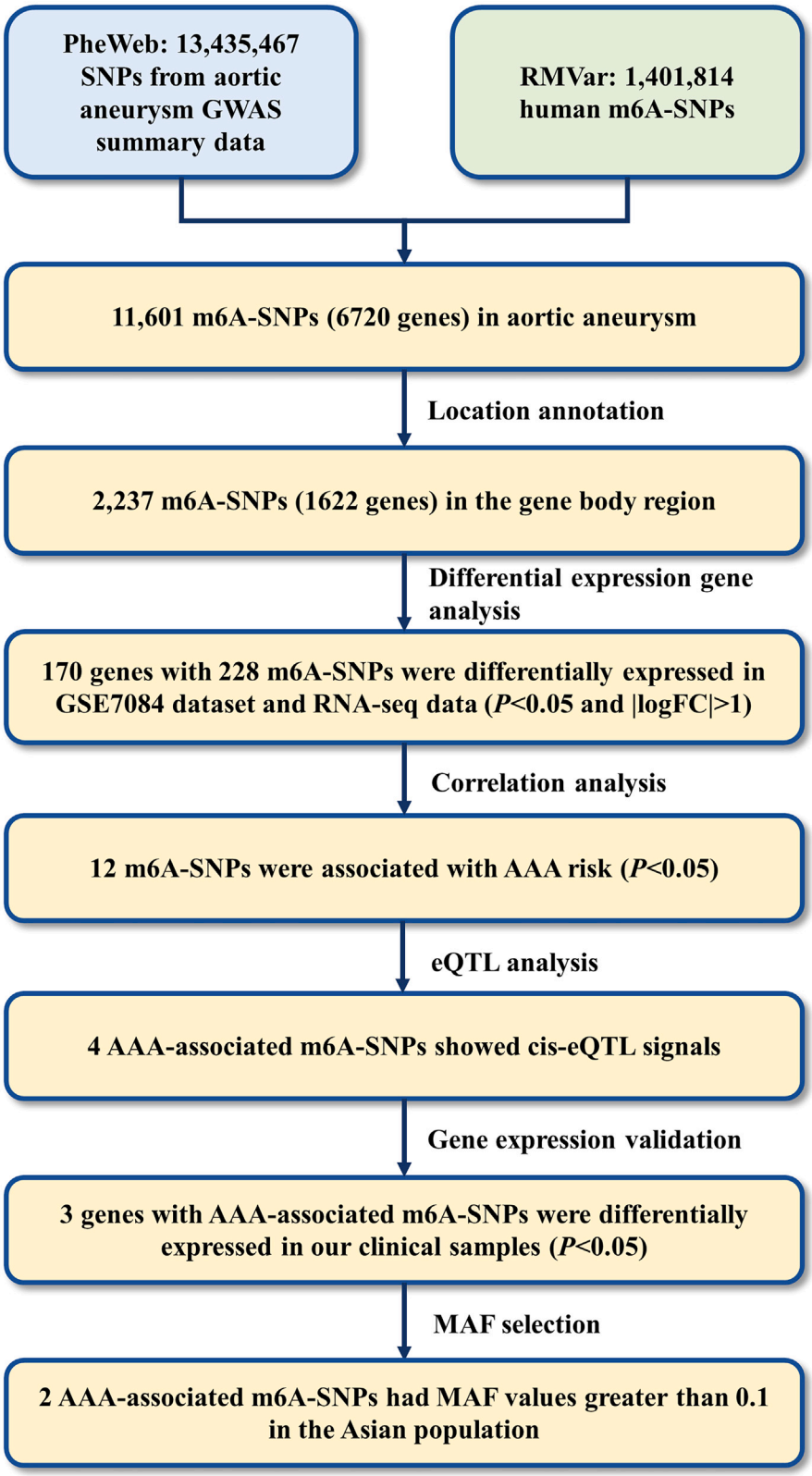

Figure 4. The screening of candidate m6A-SNPs associated with AAA risk, which introduces filter criteria for each step and displays the corresponding number of SNPs

Table 2. Baseline characteristics of the study population

Variables	Controls (n = 351)	AAA (n = 351)	p value
Age, years	66.78 ± 8.55	67.82 ± 9.65	0.130
≤65years, n (%)	162 (46.2%)	142 (40.4%)	0.148
> 65years, n (%)	189 (53.8%)	209 (59.5%)	
Male, n (%)	264 (75.2%)	274 (78.1%)	0.422
Smoking, n (%)	139 (39.6%)	137 (39.0%)	0.938
Hypertension, n (%)	180 (51.3%)	221 (63.0%)	0.002
Diabetes, n (%)	52 (14.8%)	59 (16.8%)	0.535
Dyslipidemia, n (%)	138 (39.3%)	245 (69.8%)	< 0.001

(all p < 0.05). The genotypes of rs6859 and rs10198139 in control cohort followed Hardy-Weinberg equilibrium (HWE) (p > 0.05), which implied that our samples adhered to the fundamental principles of population genetics, demonstrating their representativeness and providing support for the analytical conclusions.

The results of the risk association analysis indicated that the AG genotype and dominant model of rs6859 were linked to an increased risk of AAA with ORs of 1.543 (p = 0.011, 95%CI = 1.105–2.156) and 1.544 (p = 0.009, 95%CI = 1.117–2.134), respectively, after adjusting for hypertension and dyslipidemia (Table 3). The variant AA genotype of rs10198139 enhanced the risk of AAA compared to either GG or AG + GG genotype ($P_{AA\ vs.\ GG}$ = 0.037, OR = 2.833, 95%CI = 1.065–7.532; $P_{AA\ vs.\ AG+GG}$ = 0.036, OR = 2.840, 95%CI = 1.073–7.521) (Table 3). The optimal models for rs6859 and rs10198139 were determined separately as the dominant model and recessive model according to AIC. The combined analysis of the two SNPs showed that the AA + AG genotype of rs6859, together with any genotypes of rs10198139, could increase the susceptibility to AAA (all p < 0.05) (Table 3).

We further analyzed the associations of SNPs with AAA risk stratified by possible risk factors. The results revealed that rs6859 variant genotype conferred an increased risk of AAA in subjects aged ≤65 years, female subjects, and non-smokers. Interestingly, the same trend

Table 3. Association of rs6859 and rs10198139 polymorphisms with AAA risk

			AAA vs. CON	
Genotypes	Controls	AAA	p value	OR (95%CI)
rs6859				
GG	167	136		1 (Ref)
AG	145	175	0.011	1.543 (1.105–2.156)
AA	24	25	0.200	1.522 (0.800–2.893)
AA + AG vs. GG			0.009	1.544 (1.117–2.134)
AA vs. AG + GG			0.492	1.244 (0.667–2.320)
HWE	p = 0.322			
rs10198139				
GG	238	225		1 (Ref)
AG	98	97	0.979	0.995 (0.698–1.420)
AA	6	18	0.037	2.833 (1.065–7.532)
AA + AG vs. GG			0.568	1.104 (0.785–1.553)
AA vs. AG + GG			0.036	2.840 (1.073–7.521)
HWE	p = 0.254			
rs6859&rs10198139				
GG&AG + GG	157	128		1 (Ref)
GG&AA	3	5	0.358	2.039(0.446–9.318)
AA + AG&AG + GG	166	185	0.032	1.441(1.032–2.012)
AA + AG&AA	1	7	0.033	10.463(1.207–90.717)

After adjustment for hypertension and dyslipidemia.
See also Tables S3 and S4.

Table 4. Logistic regression models for AAA prediction

	coefficient β	SE	p value	OR	95%CI
Model 1					
Hypertension	0.383	0.168	0.023	1.466	1.055–2.038
Dyslipidemia	1.307	0.167	< 0.001	3.697	2.664–5.131
Constant	−0.941	0.155	< 0.001	0.390	
Model 2					
Hypertension	0.392	0.169	0.021	1.480	1.062–2.063
Dyslipidemia	1.326	0.169	< 0.001	3.768	2.705–5.247
rs6859	0.388	0.169	0.021	1.474	1.059–2.052
rs10198139	1.222	0.608	0.044	3.395	1.031–11.175
Constant	−1.199	0.188	< 0.001	0.302	

occurred in participants with hypertension, diabetes, or dyslipidemia (all $p < 0.05$) (Table S3). As for rs10198139, it was evident that the AA genotype and recessive model were significantly correlated with an elevated risk of AAA when compared with the GG genotype among male subjects, hypertension group, non-diabetes group, and non-dyslipidemia group (all $p < 0.05$) (Table S4).

Added value of m6A-SNPs for AAA prediction

Model 1 was developed by incorporating hypertension and dyslipidemia, and then additional variables, specifically rs6859 using a dominant model and rs10198139 using a recessive model, were included to obtain Model 2 (Table 4). The AUC value represents the area under the ROC curve and serves as an evaluation metric for binary classification models. A higher AUC value is indicative of better model performance. ROC analysis revealed that Model 1 had an AUC of 0.679, with a sensitivity of 0.705 and specificity of 0.615. However, the inclusion of rs6859 and rs10198139 in Model 1 resulted in improved predictive performance for AAA risk, with an AUC of 0.694 ($p = 0.014$) (Table 5) (Figure 5).

Potential regulatory effects of m6A-SNPs on local gene expression

Regional association maps of rs6859 and rs10198139 showed that both of them possibly interacted with candidate *cis*-regulatory elements and had high transcription levels. DNase I hypersensitivity peak clusters and transcription factor ChIP-seq clusters were observed in both SNPs (Figure 6). Furthermore, based on our RNA-seq data, we conducted a screening for transcription factors binding to two SNPs and analyzed their association with local gene expression. The results revealed that transcription factors NR3C1 and SIN3A displayed binding activity with NECTIN2 at the rs6859 loci, and showed a positive correlation with the expression of NECTIN2 (NR3C1: $r = 0.797$, $p = 0.003$; SIN3A: $r = 0.748$, $p = 0.007$). In addition, rs10198139 could interact with transcription factor KDM2B, which was also positively correlated with HPCAL1 expression ($r = 0.755$, $p = 0.006$). Notably, these three transcription factors demonstrated significant differential expression between AAA and control groups (all $p < 0.05$). To further elucidate how SNP influences m6A modification, we utilized SRAMP by inputting both the reference allele sequence and the altered allele sequence. The prediction results indicated that the sequence text with the altered allele A of rs6859 exhibited a high likelihood of generating an m6A modification site, with a very high confidence level of 99% specificity (Figure 7). However, such m6A modification changes were not observed in rs10198139.

DISCUSSION

This is the first attempt to identify m6A-SNPs that may impact the risk of AAA through an integrative analysis of GWAS data, transcriptomic expression profiles, and m6A-SNP list. By combining eQTL information, functional predictions and expression validation in human AAA tissues, we provided evidence that candidate SNPs had an effect on local gene expression related to AAA risk, possibly mediated by their influence on m6A modification. Subsequently, our study in the Chinese Han ethnic group demonstrated that the NECTIN2 rs6859 and HPCAL1 rs10198139 polymorphisms contributed to AAA susceptibility and their risk genotypes interacted to increase the likelihood of AAA. The inclusion of rs6859 and rs10198139 significantly improved the accuracy of AAA risk prediction compared to the model considering only hypertension and dyslipidemia. These findings would guide precise prevention strategies and enable personalized approaches in clinical practice.

As a vital class of functional genetic variants, m6A-SNPs can affect the levels of m6A methylation and subsequent biological processes, such as gene expression control and regulation of mRNA stability and homeostasis, thereby leading to the initiation and progression of various diseases.[16,18,26] However, until now, the relationship between m6A-SNPs and AAA susceptibility has yet to be assessed. Our enrichment analysis revealed that the DEGs in which m6A-SNPs located could participate in T cell receptor signaling pathway, immune response, cell adhesion, vascular smooth muscle contraction, calcium signaling pathway, gap junction, Wnt signaling pathway et al. These predictive features are closely related to the regulation of AAA development,[27,28] indicating a connection between m6A-SNPs and biological processes or signaling pathways associated with AAA pathogenesis.

Table 5. ROC analysis to predict AAA risk

	AUC	95%CI	p value	Sensitivity	Specificity	Youden index
Model 1	0.679	0.638–0.720	< 0.001	0.705	0.615	0.320
Model 2	0.694[a]	0.654–0.735	< 0.001	0.720	0.612	0.332

[a]p = 0.014 for comparison with Model 1.

To identify m6A-SNPs that may influence the risk of AAA and evaluate their effects on corresponding gene expression in AAA disease, we carried out this study to generate post-transcriptional m6A modification profiles through a joint analysis of GWAS data, transcriptome data, m6A-SNP list, and gene expression verification. We found that three m6A-SNPs, displaying *cis*-eQTL signals, were correlated with the susceptibility of AAA by altering the expression of local genes that were upregulated in human AAA tissues: rs7309458 in OSBPL8, rs6859 in NECTIN2, and rs10198139 in HPCAL1. Among them, rs6859 and rs10198139 had an MAF>0.1 in the Asian population. Furthermore, we genotyped these two m6A-SNPs in a Chinese Han population and confirmed that rs6859 AG genotype and dominant model, as well as rs10198139 AA genotype and recessive model, were evidently in relation to an increased risk of AAA in both overall and stratified analyses. As AAA is a complicated disease involving multiple genes and steps, we observed an obvious interaction between rs6859 and rs10198139, where carrying rs6859 AA + AG genotype together with AG + GG or AA genotype of rs10198139 was correlated with an increased risk of AAA. The synergistic effects of NECTIN2 and HPCAL1 risk variants on AAA risk may be partly due to their shared molecular pathways implicated in AAA pathogenic mechanisms.

Traditional risk prediction for AAA development mainly relies on cardiovascular features such as age, sex, smoking status, hypertension, and dyslipidemia, which confer an elevated risk of an individual toward AAA.[1] Interestingly, the association between SNPs and AAA risk may be more pronounced in the presence of certain confounding factors, as observed in our subgroup analyses. Based on multivariate logistic regression, we identified hypertension and dyslipidemia as independent predictors specific to AAA patients and combined them with significant SNP loci to recognize the presence of AAA. The addition of rs6859 and rs10198139 resulted in a much higher AUC than the model using hypertension and dyslipidemia alone. These results indicate that SNPs can enhance the predictive power at the genetic level, and their combined use with conventional risk factors represents a promising strategy for monitoring the occurrence of AAA.

NECTIN2 is a cell adhesion molecule involved in multiple cellular processes, including cell migration, proliferation, polarization, survival, and differentiation.[29,30] HPCAL1 has been identified as a specific autophagy receptor that promotes ferroptotic cell death by mediating the autophagic degradation of cadherin 2, thus reducing membrane tension and favoring lipid peroxidation.[31,32] Additionally, NECTIN2 plays a key role in lipid metabolism and vascular inflammation,[33] while HPCAL1 is implicated in lipid biosynthesis and cell cycle regulation.[34–36] Current study demonstrated a noteworthy upregulation in the expression of NECTIN2 and HPCAL1 in human AAA tissues compared to control

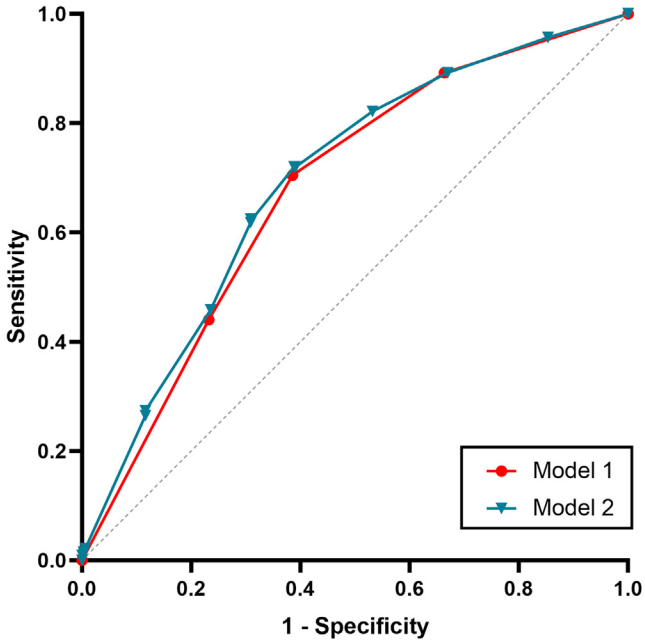

Figure 5. ROC curves of two diagnostic models

Model 2 (AUC = 0.694), which incorporates two variants, demonstrates superior diagnostic performance compared to Model 1 (AUC = 0.679).

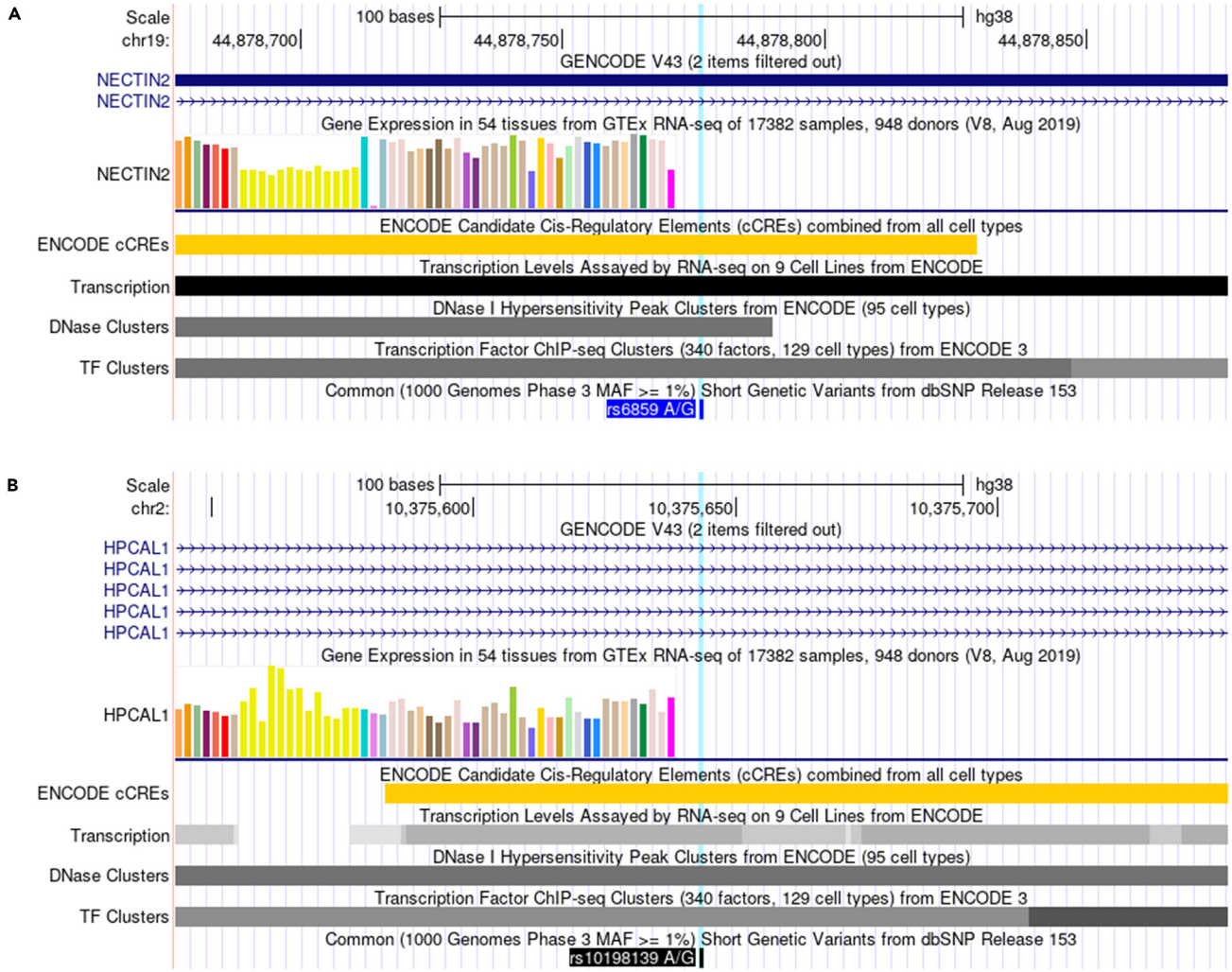

Figure 6. The regional association maps of rs6859 and rs10198139

The rs6859 (A) and rs10198139 (B) are separately located in the regulatory sequences of NECTIN2 and HPCAL1. The tracks sequentially exhibit base position, candidate combined *cis*-regulatory elements, transcription levels, DNase I hypersensitivity peak clusters, and transcription factor ChIP-seq clusters.

aortas, implying the involvement of two genes in the process of AAA. The rs6859 locates on the sixth exon in the 3′-UTR region of NECTIN2 gene and its variants may alter the binding of RNA-binding proteins or regulatory motifs.[15] GWAS analyses have reported a distinct association between rs6859 polymorphisms and several human diseases, such as Alzheimer's disease, coronary heart disease, and multiple sclerosis.[15,37,38] The rs10198139, located in the first intron of HPCAL1, may impact the binding of regulatory elements and splicing of transcripts, but its role in disease development has not been documented. Simultaneously, rs6859 and rs10198139 may approach the DNase I hypersensitivity peak clusters and transcription factor ChIP-seq clusters. Moreover, rs6859 was predicted to alter the binding of transcription factors NR3C1 and SIN3A, and affect m6A modification with very high confidence, while rs10198139 could interact with transcription factor KDM2B. According to our RNA-seq data, three transcription factors all exhibited a positive correlation with target gene expression and were differentially expressed between AAA and control tissue samples. These characteristics suggest the regulatory effects of identified SNPs on the expression of local genes, possibly achieved by changing interactions with transcription factors via an m6A methylation mechanism. It is well-established that dyslipidemia serves as a causal risk factor for AAA, and aortic wall inflammatory response is a typical pathological hallmark of AAA. Recent research has highlighted the crucial role of autophagy and ferroptosis in the pathophysiology of AAA.[39,40] Therefore, although the biological function of NECTIN2 and HPCAL1 in AAA remains unclear, it is reasonable to support the notion that the contribution of rs6859 and rs10198139 to AAA incidence is likely mediated through their influence on the expression of NECTIN2 and HPCAL1, linked to lipotoxicity, inflammation, autophagy, or ferroptosis, with abnormal m6A methylation playing a pivotal role in this process.

Overall, our genome-wide approaches revealed a groundbreaking discovery that AAA-associated m6A-SNPs might be linked with AAA pathogenesis by influencing local gene expression through m6A modification. Further population-based study elucidated a significant

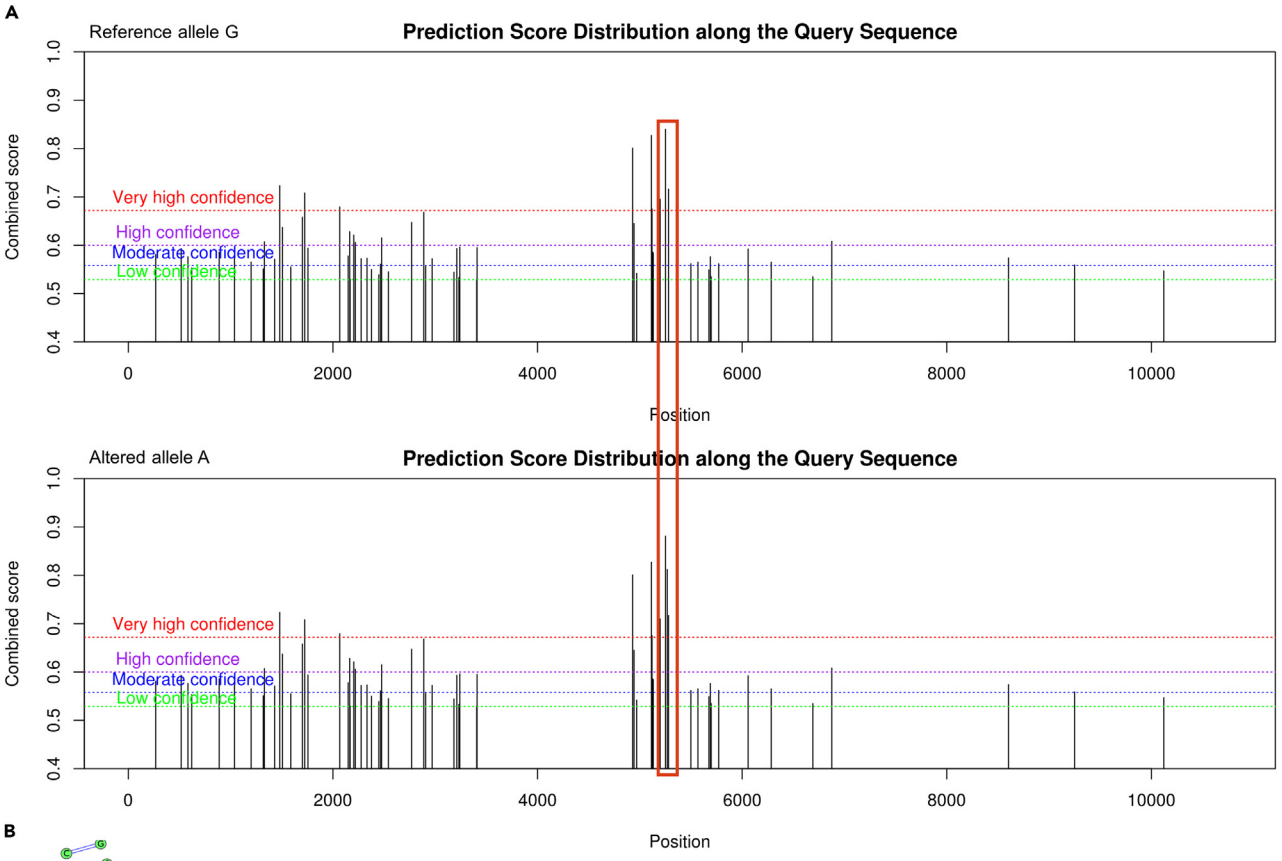

#	Position	Sequence context	Structural context	Score (binary)	Score (knn)	Score (spectrum)	Score (combined)	Decision
50	5268	TTGGG ACTTG GAGGG AGGTG GAACA GCACA CTGGA CTTCT CCCGT	BPPPP PPPPM PPPPP PPIPP MMMPP PPIII IIPPP PPPPI IIPPP	0.784	0.499	0.890	0.812	m6A site (very high confidence)

Figure 7. The m6A modification prediction for the reference allele and altered allele

(A) The red box indicates the appearance of the m6A modified peak. The horizontal axis denotes the position of the input sequence near rs6859, and the vertical axis represents the combined score. (B) Visualization of the local secondary structure around rs6859, where the m6A site demonstrates very high confidence. In the structure string, P, M, I, and B refer to paired residues, multiple loop, interior loop and bulged loop, respectively.

association between NECTIN2 rs6859 and HPCAL1 rs10198139 variants and an increased risk of AAA. Moreover, we found a potential genetic interaction between rs6859 and rs10198139 risk genotypes on elevating the incidence of AAA. By incorporating these identified m6A-SNPs, we improved the predictive value of AAA presence beyond conventional risk factors. Further studies are necessary to facilitate the clinical application and translation of these findings.

Limitations of the study

Some limitations should be addressed. First, due to the relatively low prevalence of AAA as a vascular disease, the sample size in our case-control study for verification was small. Additionally, the limited availability of human aortic histological specimens prevented us from evaluating the correlation between SNP genotyping and tissue expression of candidate genes. Second, all subjects were from Chinese Han ethnic group, and this was a single-center study. Therefore, a large-sample multicenter validation in the Asian population should be conducted to assess the generalizability and enhance the robustness of our findings. Further *in vitro* and *in vivo* experiments are required to establish the functional relevance of the identified m6A-SNPs and to confirm their impact on m6A modification, gene expression and related molecular mechanisms involved in AAA pathogenesis.

STAR★METHODS

Detailed methods are provided in the online version of this paper and include the following:

- KEY RESOURCES TABLE
- RESOURCE AVAILABILITY
  - Lead contact
  - Materials availability
  - Data and code availability
- EXPERIMENTAL MODEL AND STUDY PARTICIPANT DETAILS
  - M6A-SNP identification in aortic aneurysm
  - Differential expression analysis based on the GEO database
  - RNA sequencing (RNA-seq)
  - Functional and pathway enrichment analysis
  - eQTL analysis of m6A-SNPs
  - Prediction of m6A modification near candidate m6A-SNPs
  - DNA isolation and SNP genotyping assay
  - Total RNA extraction and quantitative real-time polymerase chain reaction (qRT-PCR)
- QUANTIFICATION AND STATISTICAL ANALYSIS

SUPPLEMENTAL INFORMATION

Supplemental information can be found online at https://doi.org/10.1016/j.isci.2024.109419.

ACKNOWLEDGMENTS

This work was supported by the National Key Research and Development Program (2022YFC2505100), Basic Scientific Research Project of Educational Department of Liaoning Province (JYTMS20230083) and National Natural Science Foundation of China (82001828).

AUTHOR CONTRIBUTIONS

T.L. conceived the study and wrote the manuscript. Y.W. analyzed the data and performed the experiments. J.Y. assisted in sample and data collection. J.J. interpreted the results. C.M. revised the manuscript. L.S. contributed to the study design and critical revision. All authors have read and approved the final version.

DECLARATION OF INTERESTS

The authors declare no conflict of interest.

Received: September 21, 2023
Revised: January 7, 2024
Accepted: March 1, 2024
Published: March 4, 2024

REFERENCES

1. Isselbacher, E.M., Preventza, O., Hamilton Black, J., 3rd, Augoustides, J.G., Beck, A.W., Bolen, M.A., Braverman, A.C., Bray, B.E., Brown-Zimmerman, M.M., Chen, E.P., et al. (2022). ACC/AHA Guideline for the Diagnosis and Management of Aortic Disease: A Report of the American Heart Association/American College of Cardiology Joint Committee on Clinical Practice Guidelines. Circulation *146*, e334–e482. https://doi.org/10.1161/CIR.0000000000001106.
2. Anagnostakos, J., and Lal, B.K. (2021). Abdominal aortic aneurysms. Prog. Cardiovasc. Dis. *65*, 34–43. https://doi.org/10.1016/j.pcad.2021.03.009.
3. Mangum, K., Gallagher, K., and Davis, F.M. (2022). The Role of Epigenetic Modifications in Abdominal Aortic Aneurysm Pathogenesis. Biomolecules *12*, 172. https://doi.org/10.3390/biom12020172.
4. Singh, T.P., Field, M.A., Bown, M.J., Jones, G.T., and Golledge, J. (2021). Systematic review of genome-wide association studies of abdominal aortic aneurysm. Atherosclerosis *327*, 39–48. https://doi.org/10.1016/j.atherosclerosis.2021.05.001.
5. Thompson, A.R., Drenos, F., Hafez, H., and Humphries, S.E. (2008). Candidate gene association studies in abdominal aortic aneurysm disease: a review and meta-analysis. Eur. J. Vasc. Endovasc. Surg. *35*, 19–30. https://doi.org/10.1016/j.ejvs.2007.07.022.
6. Lin, W., Xu, H., Wu, Y., Wang, J., and Yuan, Q. (2020). In silico genome-wide identification of m6A-associated SNPs as potential functional variants for periodontitis. J. Cell. Physiol. *235*, 900–908. https://doi.org/10.1002/jcp.29005.
7. Chasman, D.I., and Lawler, P.R. (2017). Understanding AAA Pathobiology: A GWAS Leads the Way. Circ. Res. *120*, 259–261. https://doi.org/10.1161/CIRCRESAHA.116.310395.
8. Ye, Z., Austin, E., Schaid, D.J., and Kullo, I.J. (2016). A multi-locus genetic risk score for abdominal aortic aneurysm. Atherosclerosis *246*, 274–279. https://doi.org/10.1016/j.atherosclerosis.2015.12.031.
9. Lim, C., Pratama, M.Y., Rivera, C., Silvestro, M., Tsao, P.S., Maegdefessel, L., Gallagher, K.A., Maldonado, T., and Ramkhelawon, B. (2022). Linking single nucleotide polymorphisms to signaling blueprints in abdominal aortic aneurysms. Sci. Rep. *12*, 20990. https://doi.org/10.1038/s41598-022-25144-y.
10. Oliva, M., Demanelis, K., Lu, Y., Chernoff, M., Jasmine, F., Ahsan, H., Kibriya, M.G., Chen, L.S., and Pierce, B.L. (2023). DNA methylation QTL mapping across diverse human tissues

provides molecular links between genetic variation and complex traits. Nat. Genet. *55*, 112–122. https://doi.org/10.1038/s41588-022-01248-z.

11. Brænne, I., Civelek, M., Vilne, B., Di Narzo, A., Johnson, A.D., Zhao, Y., Reiz, B., Codoni, V., Webb, T.R., Foroughi Asl, H., et al. (2015). Prediction of Causal Candidate Genes in Coronary Artery Disease Loci. Arterioscler. Thromb. Vasc. Biol. *35*, 2207–2217. https://doi.org/10.1161/ATVBAHA.115.306108.
12. Franzén, O., Ermel, R., Cohain, A., Akers, N.K., Di Narzo, A., Talukdar, H.A., Foroughi-Asl, H., Giambartolomei, C., Fullard, J.F., Sukhavasi, K., et al. (2016). Cardiometabolic risk loci share downstream cis- and trans-gene regulation across tissues and diseases. Science *353*, 827–830. https://doi.org/10.1126/science.aad6970.
13. Zhao, Y., Chen, J., Freudenberg, J.M., Meng, Q., Rajpal, D.K., and Yang, X. (2016). Network-Based Identification and Prioritization of Key Regulators of Coronary Artery Disease Loci. Arterioscler. Thromb. Vasc. Biol. *36*, 928–941. https://doi.org/10.1161/ATVBAHA.115.306725.
14. Ying, P., Li, Y., Yang, N., Wang, X., Wang, H., He, H., Li, B., Peng, X., Zou, D., Zhu, Y., et al. (2021). Identification of genetic variants in m(6)A modification genes associated with pancreatic cancer risk in the Chinese population. Arch. Toxicol. *95*, 1117–1128. https://doi.org/10.1007/s00204-021-02978-5.
15. Mo, X., Lei, S., Zhang, Y., and Zhang, H. (2019). Genome-wide enrichment of m(6)A-associated single-nucleotide polymorphisms in the lipid loci. Pharmacogenomics J. *19*, 347–357. https://doi.org/10.1038/s41397-018-0055-z.
16. Kleinbielen, T., Olasagasti, F., Azcarate, D., Beristain, E., Viguri-Díaz, A., Guerra-Merino, I., García-Orad, Á., and de Pancorbo, M.M. (2022). In silico identification and in vitro expression analysis of breast cancer-related m(6)A-SNPs. Epigenetics *17*, 2144–2156. https://doi.org/10.1080/15592294.2022.2111137.
17. Sun, X., Dai, Y., Tan, G., Liu, Y., and Li, N. (2020). Integration Analysis of m(6)A-SNPs and eQTLs Associated With Sepsis Reveals Platelet Degranulation and Staphylococcus aureus Infection are Mediated by m(6)A mRNA Methylation. Front. Genet. *11*, 7. https://doi.org/10.3389/fgene.2020.00007.
18. Edupuganti, R.R., Geiger, S., Lindeboom, R.G.H., Shi, H., Hsu, P.J., Lu, Z., Wang, S.Y., Baltissen, M.P.A., Jansen, P.W.T.C., Rossa, M., et al. (2017). N(6)-methyladenosine (m(6)A) recruits and repels proteins to regulate mRNA homeostasis. Nat. Struct. Mol. Biol. *24*, 870–878. https://doi.org/10.1038/nsmb.3462.
19. Luo, X., Li, H., Liang, J., Zhao, Q., Xie, Y., Ren, J., and Zuo, Z. (2021). RMVar: an updated database of functional variants involved in RNA modifications. Nucleic Acids Res. *49*, D1405–D1412. https://doi.org/10.1093/nar/gkaa811.
20. Zhu, R., Tian, D., Zhao, Y., Zhang, C., and Liu, X. (2021). Genome-Wide Detection of m(6)A-Associated Genetic Polymorphisms Associated with Ischemic Stroke. J. Mol. Neurosci. *71*, 2107–2115. https://doi.org/10.1007/s12031-021-01805-x.
21. Zhang, Z., Luo, K., Zou, Z., Qiu, M., Tian, J., Sieh, L., Shi, H., Zou, Y., Wang, G., Morrison, J., et al. (2020). Genetic analyses support the contribution of mRNA N(6)-methyladenosine (m(6)A) modification to human disease heritability. Nat. Genet. *52*, 939–949. https://doi.org/10.1038/s41588-020-0644-z.
22. Mo, X.B., Lei, S.F., Zhang, Y.H., and Zhang, H. (2018). Detection of m(6)A-associated SNPs as potential functional variants for coronary artery disease. Epigenomics *10*, 1279–1287. https://doi.org/10.2217/epi-2018-0007.
23. He, Y., Xing, J., Wang, S., Xin, S., Han, Y., and Zhang, J. (2019). Increased m6A methylation level is associated with the progression of human abdominal aortic aneurysm. Ann. Transl. Med. *7*, 797. https://doi.org/10.21037/atm.2019.12.65.
24. Li, K., Zhang, D., Zhai, S., Wu, H., and Liu, H. (2023). METTL3-METTL14 complex induces necroptosis and inflammation of vascular smooth muscle cells via promoting N6 methyladenosine mRNA methylation of receptor-interacting protein 3 in abdominal aortic aneurysms. J. Cell Commun. Signal. *17*, 897–914. https://doi.org/10.1007/s12079-023-00737-y.
25. Wang, K., Kan, Q., Ye, Y., Qiu, J., Huang, L., Wu, R., and Yao, C. (2022). Novel insight of N(6)-methyladenosine modified subtypes in abdominal aortic aneurysm. Front. Genet. *13*, 1055396. https://doi.org/10.3389/fgene.2022.1055396.
26. Meyer, K.D., and Jaffrey, S.R. (2014). The dynamic epitranscriptome: N6-methyladenosine and gene expression control. Nat. Rev. Mol. Cell Biol. *15*, 313–326. https://doi.org/10.1038/nrm3785.
27. Bararu Bojan Bararu, I., Pleşoianu, C.E., Badulescu, O.V., Vladeanu, M.C., Badescu, M.C., Iliescu, D., Bojan, A., and Ciocoiu, M. (2023). Molecular and Cellular Mechanisms Involved in Aortic Wall Aneurysm Development. Diagnostics *13*, 253. https://doi.org/10.3390/diagnostics13020253.
28. Quintana, R.A., and Taylor, W.R. (2019). Cellular Mechanisms of Aortic Aneurysm Formation. Circ. Res. *124*, 607–618. https://doi.org/10.1161/CIRCRESAHA.118.313187.
29. Takai, Y., Irie, K., Shimizu, K., Sakisaka, T., and Ikeda, W. (2003). Nectins and nectin-like molecules: roles in cell adhesion, migration, and polarization. Cancer Sci. *94*, 655–667. https://doi.org/10.1111/j.1349-7006.2003.tb01499.x.
30. Zhang, S., Jiang, C., Su, Y., Gui, J., Yue, Z., Jian, B., He, S., and Ma, X. (2023). Nectin2 influences cell apoptosis by regulating ANXA2 expression in neuroblastoma. Acta Biochim. Biophys. Sin. *55*, 356–366. https://doi.org/10.3724/abbs.2023020.
31. Chen, F., Cai, X., Kang, R., Liu, J., and Tang, D. (2023). Autophagy-Dependent Ferroptosis in Cancer. Antioxidants & Redox Signaling. https://doi.org/10.1089/ars.2022.0202.
32. Chen, X., Song, X., Li, J., Zhang, R., Yu, C., Zhou, Z., Liu, J., Liao, S., Klionsky, D.J., Kroemer, G., et al. (2023). Identification of HPCAL1 as a specific autophagy receptor involved in ferroptosis. Autophagy *19*, 54–74. https://doi.org/10.1080/15548627.2022.2059170.
33. Rossignoli, A., Shang, M.M., Gladh, H., Moessinger, C., Foroughi Asl, H., Talukdar, H.A., Franzén, O., Mueller, S., Björkegren, J.L.M., Folestad, E., and Skogsberg, J. (2017). Poliovirus Receptor-Related 2: A Cholesterol-Responsive Gene Affecting Atherosclerosis Development by Modulating Leukocyte Migration. Arterioscler. Thromb. Vasc. Biol. *37*, 534–542. https://doi.org/10.1161/ATVBAHA.116.308715.
34. Chen, T., Yuan, Z., Lei, Z., Duan, J., Xue, J., Lu, T., Yan, G., Zhang, L., Liu, Y., Li, Q., and Zhang, Y. (2022). Hippocalcin-Like 1 blunts liver lipid metabolism to suppress tumorigenesis via directly targeting RUVBL1-mTOR signaling. Theranostics *12*, 7450–7464. https://doi.org/10.7150/thno.75936.
35. Wang, X., Xie, X., Zhang, Y., Ma, F., Pang, M., Laster, K.V., Li, X., Liu, K., Dong, Z., and Kim, D.J. (2022). Hippocalcin-like 1 is a key regulator of LDHA activation that promotes the growth of non-small cell lung carcinoma. Cell. Oncol. *45*, 179–191. https://doi.org/10.1007/s13402-022-00661-0.
36. Zhang, Y., Liu, Y., Duan, J., Yan, H., Zhang, J., Zhang, H., Fan, Q., Luo, F., Yan, G., Qiao, K., and Liu, J. (2016). Hippocalcin-like 1 suppresses hepatocellular carcinoma progression by promoting p21(Waf/Cip1) stabilization by activating the ERK1/2-MAPK pathway. Hepatology *63*, 880–897. https://doi.org/10.1002/hep.28395.
37. Mizutani, K., Miyata, M., Shiotani, H., Kameyama, T., and Takai, Y. (2022). Nectin-2 in general and in the brain. Mol. Cell. Biochem. *477*, 167–180. https://doi.org/10.1007/s11010-021-04241-y.
38. Xiao, Q., Xi, J., Wang, R., Zhao, Q., Liang, X., Wu, W., Zheng, L., Guo, Q., Hong, Z., Fu, H., and Ding, D. (2022). The Relationship Between Low-Density Lipoprotein Cholesterol and Progression of Mild Cognitive Impairment: The Influence of rs6859 in PVRL2. Front. Genet. *13*, 823406. https://doi.org/10.3389/fgene.2022.823406.
39. Zhang, Y., Xin, L., Xiang, M., Shang, C., Wang, Y., Wang, Y., Cui, X., and Lu, Y. (2022). The molecular mechanisms of ferroptosis and its role in cardiovascular disease. Biomedicine & pharmacotherapy = Biomedecine & pharmacotherapie *145*, 112423. https://doi.org/10.1016/j.biopha.2021.112423.
40. Wang, L., Liu, S., Pan, B., Cai, H., Zhou, H., Yang, P., and Wang, W. (2020). The role of autophagy in abdominal aortic aneurysm: protective but dysfunctional. Cell Cycle *19*, 2749–2759. https://doi.org/10.1080/15384101.2020.1823731.

STAR★METHODS

KEY RESOURCES TABLE

REAGENT or RESOURCE	SOURCE	IDENTIFIER
Biological samples		
DNA and RNA from AAA patients and controls	The First Hospital of China Medical University	
Chemicals, peptides, and recombinant proteins		
TRIZOL Reagent	Thermo Fisher Scientific	Cat#15596026
Isopropanol	MACKLIN	Cat#I811925
Ethanol	Hushi	Cat#10009218
StarScript III Reverse Transcriptase	GenStar	Cat#A231
SYBR PCR reagent	Vazyme Biotechnology	Cat#Q711
Critical commercial assays		
Kompetitive Allele Specific PCR (KASP)	Baygene Biotechnology Company Limited (Shanghai, China)	
RNA sequencing	Novogene Bioinformatics Technology Co. (Beijing, China)	
Deposited data		
GWAS summary data for aortic aneurysm	PheWeb	https://pheweb.jp/
RNA modification associated variants database	RMVar	https://rmvar.renlab.org/
Transcriptomic expression profile data	GEO database	GSE7084; RRID:SCR_005012
eQTL analysis	VannoPortal	http://www.mulinlab.org/vportal/index.html
Functions of SNPs	VannoPortal	http://www.mulinlab.org/vportal/index.html
Regional association maps	UCSC Genome Browser	https://genome.ucsc.edu/; RRID:SCR_005780
M6A modification prediction of SNPs	SRAMP	https://www.cuilab.cn/sramp; RRID:SCR_024500
Oligonucleotides		
Primers for OSBPL8, see Table S1	This paper	
Primers for ZNF12, see Table S1	This paper	
Primers for NECTIN2, see Table S1	This paper	
Primers for HPCAL1, see Table S1	This paper	
Primers for β-actin, see Table S1	This paper	
Software and algorithms		
R package qqman	RRID:SCR_024293	https://github.com/stephenturner/qqman
R package org.Hs.eg.db		https://www.bioconductor.org/packages/org.Hs.eg.db/
R package clusterProfiler	RRID:SCR_016884	https://bioconductor.org/packages/clusterProfiler/
R package limma	RRID:SCR_010943	https://bioconductor.org/packages/release/bioc/html/limma.html
GEO2R	RRID:SCR_016569	https://www.ncbi.nlm.nih.gov/geo/geo2r/
KEGG rest API		https://www.kegg.jp/kegg/rest/keggapi.html
SPSS 23.0		https://www.ibm.com/cn-zh
MedCalc Version 20.218		https://www.medcalc.org/

RESOURCE AVAILABILITY

Lead contact

Further information and requests for resources and reagents should be directed to and will be fulfilled by the lead contact, Liping Sun (lpsun@cmu.edu.cn).

Materials availability

This study did not generate new reagents or materials.

Data and code availability

- This paper analyzes existing GWAS summary data, RNA modification associated variants, transcriptomic expression profile data, eQTL data, functions of SNPs, regional association maps and M6A modification prediction of SNPs from publicly available databases. These accession numbers for the databases are listed in the key resources table.
- This paper does not report original code.
- Any additional information required to reanalyze the data reported in this paper is available from the leading contact upon request.

EXPERIMENTAL MODEL AND STUDY PARTICIPANT DETAILS

All participants were enrolled from the First Hospital of China Medical University between August 2017 and July 2020. Our case-control cohort comprised a total of 351 pairs of Chinese Han ethnic AAA patients and controls matched by age and sex (Average age: 67.30 $\pm$ 9.12 years; Male: 538 (76.6%)). The cases were recruited from the vascular surgery department and diagnosed via computed tomography angiography. All controls were from the physical examination center and underwent imaging examination to exclude AAA within the last two weeks of recruitment. Participants who had Marfan syndrome, previous aortic surgery, traumatic AAA, malignant tumors, hematological diseases, infectious diseases, autoimmune diseases or severe organ failure were excluded. A fasting venous blood sample of 5 mL was taken from each subject, and baseline information including age, sex, smoking status, hypertension, diabetes and dyslipidemia was collected from medical records. Aneurysmal abdominal aortic tissues from seven AAA patients who underwent open surgical repair and normal abdominal aortas from five organ donors who underwent kidney transplantation were obtained for RNA-seq, and additional seven AAA tissue samples and five control aortas were collected for qRT-PCR. This study was approved by the Ethics Committee of the First Hospital of China Medical University (Shenyang, China, Ethical Approval Number: [2020]146) and informed consent was obtained from all subjects involved in the study.

M6A-SNP identification in aortic aneurysm

We initially downloaded GWAS data for aortic aneurysm from PheWeb (https://pheweb.jp/), a database consisting of GWAS summary statistics from the BioBank Japan Project (BBJ) which included 1,155 cases and 173,601 controls. RMVar (https://rmvar.renlab.org/) is a published RNA modification (RM) database that contains a total of 1,678,126 RM-associated variants for nine kinds of modification, including m6A, m6A.m., m1A, pseudouridine, m5C, m5U, 2′-*O*-Me, A-to-I and m7G, at three confidence levels. Then, a list of human SNPs that could influence m6A modification was downloaded from RMVar and intersected with the GWAS summary data. The Manhattan plot was generated by the R package "qqman" to show the location and *p* value of each SNP. SNPs with a p-value $<$ 0.05 in the GWAS summary data were considered to be associated with the disease.

Differential expression analysis based on the GEO database

To determine whether the local genes of m6A-SNPs were differentially expressed between human AAA and normal aortic tissues, transcriptomic expression profile data were downloaded from the GSE7084 dataset which included 2 AAA cases and 2 controls in the GEO database (http://www.ncbi.nlm.nih.gov/geo). GEO2R tool, based on the "limma" package in R, was used to analyze differential gene expression on the GPL570 platform. And genes with a p-value $<$ 0.05 and $|logFC| > 1$ were considered as differentially expressed genes (DEGs).

RNA sequencing (RNA-seq)

RNA extraction from abdominal aortas was conducted and followed by quality inspection. The NEBNext UltraTM RNA Library Prep Kit from Illumina was utilized for library construction. Preliminary quantification was carried out using the Qubit 2.0 Fluorometer. After successful library quality assessment, sequencing was performed on the high-throughput Illumina NOVA6000 platform. The image data obtained from the sequencer underwent processing through CASAVA for base calling, generating sequence data (reads). HISAT2 v2.0.5 was used to build an index of the reference genome, aligning paired-end clean reads to the reference genome. FeatureCounts (1.5.0-p3) was employed to calculate read counts mapped to each gene. The data were normalized to $\log_2$(TPM+0.0001) format, and differential gene expression analysis was conducted using the "limma" package. Genes with a p-value $<$ 0.05 and $|logFC| > 1$ were deemed statistically significant.

Functional and pathway enrichment analysis

For gene ontology (GO) and kyoto encyclopedia of genes and genomes (KEGG) analysis, we utilized gene annotations from the R package org.Hs.eg.db (version 3.1.0) for GO annotations, and KEGG rest API (https://www.kegg.jp/kegg/rest/keggapi.html) for KEGG pathway annotations. DEGs were mapped to the background set. Enrichment analysis was performed using the R package clusterProfiler (version 3.14.3) to obtain results of gene set enrichment. A minimum gene set size of 5 was established, and statistical significance was determined with a threshold of p $<$ 0.05 and false discovery rate (FDR) $<$ 0.1.

eQTL analysis of m6A-SNPs

To identify m6A-SNPs associated with changes in local gene expression, we utilized the VannoPortal database (http://www.mulinlab.org/vportal/index.html) to assess whether m6A-SNPs displayed eQTL signals ($p < 0.05$). In addition, the possible functions of m6A-SNPs in the process of transcriptional regulation such as transcription factor binding, motifs changed and histone modification were determined by VannoPortal. Regional association maps of candidate m6A-SNPs were generated using UCSC Genome Browser (https://genome.ucsc.edu/).

Prediction of m6A modification near candidate m6A-SNPs

Sequence-based RNA adenosine methylation site predictor (SRAMP) is an online tool designed for predicting m6A modification by analyzing genomic sequences within a machine learning framework (http://www.cuilab.cn/sramp/). By inputting sequences with reference allele and altered allele, we can determine whether m6A-SNPs affect the surrounding m6A modification. The tool classifies m6A sites with very high, high, moderate or low confidence according to the thresholds that achieve 99%, 95%, 90% and 85% specificities, respectively.

DNA isolation and SNP genotyping assay

Blood samples were centrifuged for 10 min at 3500 r/min and 4°C, and clots were isolated and stored at −80°C. Total DNA was extracted from each blood clot following a standard phenol-chloroform procedure. Genotyping assays were performed by Baygene Biotechnology Company Limited (Shanghai, China) using Kompetitive Allele Specific PCR (KASP) method on the SNPLine platform (LGC, United Kingdom). The detail of KASP method included primer design, PCR amplification, competitive amplification, fluorescence detection and data analysis. To ensure the reliability and accuracy of genotyping assays, we strictly followed the procedure for quality control. The DNA sample concentration was greater than 50 ng/ul, and the purity (260/280 ratio) was between 1.7 and 1.9. The genotyping rate of the primer test should be greater than 90%. If it was less than 90%, the primer should be replaced and retested until it met the requirement. Around 10% of random DNA samples were re-genotyped to ensure genotyping reproducibility and the concordance rate was 100%. SNPs with a call rate less than 90% were excluded.

Total RNA extraction and quantitative real-time polymerase chain reaction (qRT-PCR)

Total RNA from abdominal aortic tissues was extracted using TRIZOL Reagent (Thermo Fisher Scientific, Waltham, USA). The homogenized tissue was mixed with Trizol, and chloroform was added to the mixture. The upper aqueous phase was collected, and isopropanol (MACKLIN-I811925, Shanghai, China) was added. After centrifugation, the supernatant was discarded, and the RNA precipitate was washed with 75% ethanol (Hushi-10009218, Shanghai, China). The RNA was then air-dried and dissolved in nuclease-free water. It was stored at −80°C for preservation.

The extracted RNA was reverse transcribed into cDNA utilizing StarScript III Reverse Transcriptase (GenStar, Beijing, China), and the cDNA was stored at −20°C for further use. To measure the relative mRNA expression of target genes, qRT-PCR was performed using SYBR PCR reagent (Vazyme Biotechnology, Nanjing, China). The reaction mixture included 10 μl of SYBR qPCR Master Mix, 0.4 ul of forward primer, 0.4 ul of reverse primer, 8.2 ul of enzyme-free water and 1.0 ul of cDNA. The thermal cycling protocol consisted of an initial denaturation at 95°C for 1 minute, followed by 40 cycles of denaturation at 95°C for 10 seconds, annealing at 60°C for 30 seconds, and extension, followed by a melting curve analysis. The gene expression levels were calculated using the $2^{-\Delta\Delta ct}$ method, with β-actin serving as the internal control. The primer information is provided in Table S1.

QUANTIFICATION AND STATISTICAL ANALYSIS

All data were statistically analyzed with SPSS 23.0 software. The Student's *t* test or Mann-Whitney U-test was used to compare continuous variables, and chi-square (χ^2) test was employed to compare categorical variables. Logistic regression was applied to estimate the odds ratio (OR) and 95% confidence interval (CI) for the relationship between candidate m6A-SNPs and AAA risk, as well as to construct prediction models. The receiver operating characteristic (ROC) curves were conducted to evaluate the model's diagnostic efficacy by calculating the area under the ROC curve (AUC), sensitivity and specificity. Additionally, pairwise comparison of ROC curves was performed using MedCalc Version 20.218. p value <0.05 was considered statistically significant. The optimal genetic model for each m6A-SNP was determined using the Akaike information criterion (AIC). The dominant and recessive models were defined as heterozygote+homozygote variant vs. homozygote wild and homozygote variant vs. heterozygote+homozygote wild, respectively.